CU-LTE: Spectrally-Efficient and Fair Coexistence Between LTE and Wi-Fi in Unlicensed Bands

Zhangyu Guan and Tommaso Melodia
Department of Electrical and Computer Engineering
Northeastern University, MA 02115, USA
Email:{zguan, melodia}@ece.neu.edu

***Abstract*—To cope with the increasing scarcity of spectrum resources, researchers have been working to extend LTE/LTE-A cellular systems to unlicensed bands, leading to so-called *unlicensed LTE* (U-LTE). However, this extension is by no means straightforward, primarily because *the radio resource management schemes* used by LTE and by systems already deployed in unlicensed bands are *incompatible*. Specifically, it is well known that coexistence with scheduled systems like LTE degrades considerably the throughput of Wi-Fi networks that are based on carrier-sense medium access schemes.**

To address this challenge, we propose for the first time a cognitive coexistence scheme to enable spectrum sharing between U-LTE and Wi-Fi networks, referred to as CU-LTE. The proposed scheme is designed to jointly determine dynamic channel selection, carrier aggregation and fractional spectrum access for U-LTE networks, while guaranteeing fair spectrum access for Wi-Fi based on a newly designed cross-technology fairness criterion. We first derive a mathematical model of the spectrum sharing problem for the coexisting networks; we then design a solution algorithm to solve the resulting fairness constrained mixed integer nonlinear optimization problem. The algorithm, *based on a combination of branch and bound and convex relaxation techniques*, maximizes the network utility with guaranteed optimality precision that can be set arbitrarily to 1 at the expense of computational complexity. Performance evaluation indicates that near-optimal spectrum access can be achieved with guaranteed fairness between U-LTE and Wi-Fi. Issues regarding implementation of CU-LTE are also discussed.

***Index Terms*—LTE/LTE-A, Wi-Fi, Unlicensed Spectrum Band, Cognitive Spectrum Access.**

I. Introduction

With the ongoing deployment of LTE and LTE-Advanced cellular systems (hereafter LTE for conciseness), an increasing number of smartphones are reaching the market every year. As smartphone penetration has resulted in drastic increase in cellular network traffic loads, service providers (SPs) are facing the challenge of scarce spectrum resources (mainly between 700 MHz and 2.6 GHz [1]). As a possible solution to this problem, leading manufacturers (including Qualcomm, Ericsson and Huawei, among others) and SPs (like Verizon and China Mobile) have considered extending the new-generation of LTE systems to unlicensed bands (2.4 and 5 GHz) to leverage additional spectrum resources, leading to so-called unlicensed LTE (U-LTE) [2], [3]. U-LTE will operate pico/femto cells in unlicensed bands with transmission power levels much lower than typically used in macro cells.

However, extending LTE to unlicensed bands is by no means trivial, primarily because of the *lack of compatibility between the radio resource management (RRM) schemes* used by LTE and by systems already deployed in unlicensed band (e.g., Wi-Fi). The underlying RRM policy of LTE systems is in fact based on centralized scheduling on each LTE base station (referred to as eNodeB). This is different from typical systems with distributed control that are already deployed in unlicensed bands, e.g., IEEE 802.11-based (Wi-Fi) systems with RRM based on distributed coordination function (DCF) running in all wireless stations (STAs). It has been observed that the throughput of Wi-Fi systems can be considerably degraded (more than 50% under high traffic loads) in the presence of co-channel interference from LTE systems [3], [4], which is not desirable especially for SPs who have deployed tens of thousands of Wi-Fi hotspots over the world.

To date, there is still no widely accepted coexistence scheme to enable spectrally-efficient and fair spectrum sharing between LTE and Wi-Fi, with the exception of a few recent research efforts. For example, Huawei and Qualcomm proposed to deploy U-LTE in only partially unlicensed bands (say $5.725\sim5.825$ GHz) and areas with sparse Wi-Fi deployments [2], [3]. The limitation of this approach is that it may lead to under-utilization of spectrum resources compared to exploiting the whole unlicensed band. In [4], [5] the authors proposed to enable coexistence of U-LTE and Wi-Fi by taking advantage of the so-called Almost Blank Subframe (ABSF), a time-domain multiplexing feature in 3GPP Rel. 10 [1]. The challenge there, as pointed out in [5], is how to find the optimal operating point between the air time given up by LTE and the throughput achievable by the Wi-Fi networks. Without a properly defined fairness criterion for spectrum sharing, Wi-Fi networks may get completely stalled if the co-located LTE networks selfishly offload too much traffic to the unlicensed bands.

To address this challenge, in this article we focus on designing a new coexistence scheme to enable spectrally-efficient spectrum sharing between LTE and Wi-Fi networks deployed in the same unlicensed bands while guaranteeing fairness between them. Our main contributions are as follows:

- **Architecture design**: We present for the first time cognitive unlicensed LTE (CU-LTE), a cognitive coexistence architecture to enable distributed spectrum sharing between LTE and Wi-Fi networks on the same unlicensed bands. The architecture jointly determines dynamic channel selection (*which channels to use?*), carrier aggregation (*how many channels to use?*), and fractional spectrum access (*how frequently to access the channel?*) for LTE networks, while guaranteeing fair spectrum access for Wi-Fi based on cognitively sensing the Wi-Fi traffic

This work was supported in part by the Air Force Research Laboratory under Contract FA8750-14-1-0074, and by the National Science Foundation under Grant CNS-1218717.

load level and on a newly designed cross-technology fairness criterion. The fairness criterion ensures that the performance degradation caused by an unlicensed LTE Pico cell to the Wi-Fi network is no more than the performance degradation that would be caused by another co-located Wi-Fi.

- **Modeling and optimization**: Based on the designed coexistence architecture, we model the spectral efficiency of the coexisting networks and propose algorithms to maximize it. First, we derive a mathematical model of the spectrum sharing problem for the coexisting U-LTE/Wi-Fi networks, and design a solution algorithm to solve the resulting fairness-constrained mixed integer nonlinear optimization problem. The algorithm is based on a combination of branch and bound and convex relaxation techniques, with the objective to maximize the aggregate utility of the LTE networks to achieve certain predefined optimality precision while guaranteeing fairness to the Wi-Fi networks. The optimality precision can be set as close to 1 as we wish, with a resulting tradeoff between utility optimality and computational complexity.
- **Performance evaluation**: The performance of the coexisting U-LTE/Wi-Fi networks is analyzed based on the optimization results. We show that the CU-LTE coexistence scheme achieves nearly optimal spectrum assignment for U-LTE while guaranteeing fair coexistence between U-LTE and Wi-Fi in a diverse set of network settings. Issues regarding practical applicability of the coexistence scheme are also discussed, with technologies envisioned to enable cognitive coexistence that requires *no* signaling exchange between U-LTE and Wi-Fi.

Compared to existing research efforts [4]–[9], the proposed CU-LTE coexistence scheme can enable i) *spectrally-efficient coexistence* between U-LTE and Wi-Fi *without* restricting the deployment of U-LTE to certain unlicensed bands, hence allowing LTE networks to optimize their spectral efficiency through dynamic spectrum access; ii) *fair coexistence* between U-LTE and Wi-Fi networks based on a new cross-technology fairness criterion; and finally iii) *cognitive coexistence* so that the resulting spectrum sharing does not require any changes to the protocol stack of already deployed Wi-Fi networks.

The remainder of the paper is organized as follows. In Section II, we review related work. In Section III we present the coexistence architecture with the newly designed cross-technology fairness criterion presented in Section IV. In Section V we describe the network utility maximization algorithm, and show the performance evaluation results in Section VI. Applicability issues are discussed in Section VII, and finally we draw main conclusions in Section VIII.

II. Related Work

Previous work has addressed radio resource management (RRM) in heterogeneous wireless networks, including multi-tier LTE networks [10]–[12], cross-technology RRM in unlicensed band [13]–[15] and RRM between U-LTE and Wi-Fi networks [4]–[9].

RRM in Multi-tier LTE. In multi-tier LTE networks, Macro, Micro, Pico, and Femtocells coexist and operate on the same or on partially overlapped spectrum bands dedicated to the SP. Different RRM schemes have been discussed for intra- and inter-tier interference mitigation based on resource (i.e., power, frequency and time) negotiation among neighbour cells [10]. Čierny et al. modeled in [11] the cross-tier interference based on stochastic geometry theory in two-tier (Macro/Femto and Macro/Pico) LTE networks, and showed that more balanced throughput can be achieved by jointly assigning almost blank subframes between the tiers. A good survey for RRM in LTE networks can be found in [12]. In unlicensed bands, resource negotiation is not always feasible, e.g., because of commercial conflicts among SPs deploying the systems. since coexisting systems may be deployed by the same or different SPs.

Cross-technology RRM. Coexistence schemes have long been studied considering cross-technology wireless systems. For example, Chiasserini et al. proposed in [13] two coexistence schemes between WLAN and Bluetooth systems in 2.4 GHz ISM Band, with and without relying on cross-system signaling exchange, respectively. Zhang et al. proposed in [14] "cooperative busy tone" to improve the probability that a ZigBee network is visible to coexisting Wi-Fi networks, while in [15] Guo et al. enhanced the ZigBee throughput in the presence of Wi-Fi interference based on adaptive forward error-correction coding. Compared to Bluetooth and ZigBee, the transmission power of LTE PeNBs can be much higher (typically around 20 dBm against 5 dBm for Bluetooth and 0 dBm for ZigBee). Consequently, Wi-Fi becomes the victim in coexisting LTE and Wi-Fi networks due to its DCF-based channel access.

Coexisting U-LTE and Wi-Fi. Works [4]–[9] are the most closely related to ours. In [6], Ratasuk et al. proposed a listen-before-talk scheme by enabling carrier sensing at each LTE PeNB. While the scheme can enable fair coexistence between U-LTE and Wi-Fi, it results in spectrum underutilization because of the carrier sense operation in the listen-before-talk. Almeida et al. showed [4], [5] that without proper ABSF assignment for the coexisting U-LTE networks, the throughput of Wi-Fi networks can be significantly degraded; similar considerations were reported in [7]. In recent work [8], Sagari proposed an inter-network coordination architecture to enable dynamic interference management between coexisting U-LTE and Wi-Fi networks. Different from these works, which focused on simulation-based performance analysis and coordinated RRM, in this work we focus on cognitive (i.e., without direct message exchange) and distributed coexistence between U-LTE and Wi-Fi; specifically, we focus on optimizing the spectral efficiency of LTE networks while guaranteeing fairness between LTE and Wi-Fi. In [9], Yun et al. proposed an LTE/Wi-Fi coexistence scheme by allowing LTE and WiFi to transmit together and decode the interfered signals. The scheme requires to redesign the physical-layer protocol stack for both LTE and Wi-Fi networks. Differently, our coexistence scheme is backward compatible with currently deployed Wi-Fi networks and is "cognitive", in the sense that it requires *no* signaling exchange between co-located LTE and Wi-Fi.

III. Coexistence Architecture

We consider coexisting LTE and Wi-Fi networks, where there is one LTE Macro cell eNodeB, a set $\mathcal{M}$ of LTE PeNBs, and a set $\mathcal{N}$ of Wi-Fi Access Points (APs). Denote the set of LTE User Equipments (UEs) served by each PeNB $m \in \mathcal{M}$ as $\mathcal{L}_m$, and the set of Wi-Fi Stations associated to AP $n \in \mathcal{N}$ as $\mathcal{W}_n$. The coexistence architecture is designed following a Licensed-Assisted Access (LAA) operation mode. That is, the LTE Macro eNodeB operates in a licensed band to transmit critical information (e.g., downlink/uplink control information for authentication, scheduling and handover, among others) and to guarantee Quality of Service (QoS) of UEs. The PeNBs operate in the licensed band for uplink transmissions and in the unlicensed band to boost the downlink data rate based on *multi-channel fractional spectrum access (FSA)*. The communications of Macro eNodeB and PeNBs are coordinated via wideband backbone networks. The objective of the coexistence architecture design is to achieve spectrally-efficient channel access for LTE networks while guaranteeing fairness between LTE and Wi-Fi networks.

A. Multi-Channel Fractional Spectrum Access

The core idea of fractional spectrum access is to mute or limit the transmission (i.e., with zero or reduced transmission power) of LTE networks such that LTE accesses a channel in a fractional portion of air time only. This can be accomplished in each PeNB by transmitting frequently so-called Almost-blank Subframes (ABSFs), which is a feature introduced in 3GPP Rel. 10 for enhanced Inter-Cell Interference Coordination (eICIC) [1]. ABSF are special LTE subframes in which a PeNB does not send any data and instead sends only control signals at much lower power and of shorter duration than normal subframes. Consequently, the corresponding channel will be sensed idle and accessed by the coexisting Wi-Fi networks. For example, as shown in Fig. 1, by scheduling five ABSFs during an LTE frame (which includes 10 subframes) the PeNB accesses the channel for approximately 50% of the air time (against 100% in a normal LTE frame) while leaving the other 50% of the time available for Wi-Fi. The more ABSFs are scheduled in a frame by an LTE PeNB, the more transmission opportunities are left for Wi-Fi networks.

Multi-channel FSA. Consider unlicensed spectrum bands that are divided into a set $\mathcal{F}$ of non-overlapped channels; for example, channels 1, 6, 11 in the 2.4 GHz band and channels $36, 40, 44, \cdots, 64$ in 5 GHz band. Let $f_n \in \mathcal{F}$ denote the channel selected by Wi-Fi network $n \in \mathcal{N}$. Then, our objective is to assign one or more channels (i.e., with carrier aggregation enabled) to each PeNB $m \in \mathcal{M}$ and decide how frequently PeNB m should access each of the assigned channels.

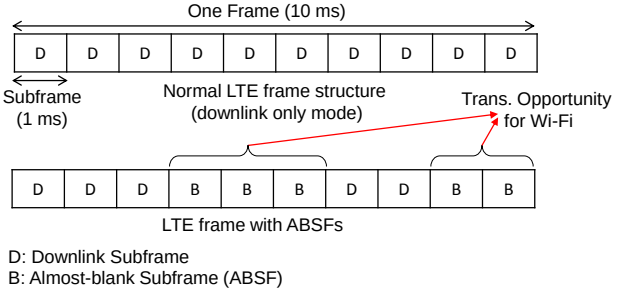

Fig. 1: LTE frame with Almost-blank Subframes (ABSFs).

Let $\boldsymbol{\alpha} \triangleq (\alpha_{mf})_{m\in\mathcal{M}}^{f\in\mathcal{F}}$ represent the channel assignment profile, with $\alpha_{mf} = 1$ if channel f is assigned to PeNB $m \in \mathcal{M}$, and $\alpha_{mf} = 0$ otherwise, i.e.,

$$\alpha_{mf} \in \{0,\ 1\},\ \forall m \in \mathcal{M},\ f \in \mathcal{F}. \tag{1}$$

Let $F_{\max}$ denote the maximum number of channels that each PeNB is allowed to operate on simultaneously. Then, we have

$$\sum_{f\in\mathcal{F}} \alpha_{mf} \le \min(F_{\max},\ |\mathcal{F}|),\ \forall m \in \mathcal{M}, \tag{2}$$

where $|\mathcal{F}|$ is the cardinality of channel set $\mathcal{F}$. Here, $F_{\max}$ can be determined according to the signal processing capabilities of each PeNB and to achieve a tradeoff between spectrum utilization efficiency and signal processing and signaling overhead.

Further denote $\boldsymbol{\beta} \triangleq (\beta_{mf})_{m\in\mathcal{M}}^{f\in\mathcal{F}}$ as the FSA profile, where $\beta_{mf} \in [0,\ 1]$ is the percentage of air time during which PeNB $m \in \mathcal{M}$ accesses channel f. Then, we have

$$\beta_{mf} \ge 0,\ \forall m \in \mathcal{M},\ f \in \mathcal{F}, \tag{3}$$

$$\beta_{mf} \le 1,\ \forall m \in \mathcal{M},\ f \in \mathcal{F}, \tag{4}$$

$$\beta_{mf} \le \alpha_{mf},\ \forall m \in \mathcal{M},\ f \in \mathcal{F}, \tag{5}$$

where (5) implies that PeNB m is not allowed to access channel f if the latter is not assigned to PeNB m.

Let $R_m(\boldsymbol{\alpha}, \boldsymbol{\beta})$ represent the throughput achievable by PeNB $m \in \mathcal{M}$. Then, our objective in designing the coexistence architecture is to maximize the utility of LTE networks while guaranteeing certain predefined cross-technology fairness criterion $\Gamma_{\text{l-w}}$ between LTE and Wi-Fi networks, i.e.,

$$\begin{array}{ll} \text{Given}: & \mathcal{M}, \mathcal{N}, \mathcal{L}_m, \mathcal{W}_n, \Gamma_{\text{l-w}}, m \in \mathcal{M}, n \in \mathcal{N} \\ \underset{\boldsymbol{\alpha},\,\boldsymbol{\beta}}{\text{Maximize}} & U \triangleq \sum\limits_{m\in\mathcal{M}} U_m\big(R_m(\boldsymbol{\alpha},\ \boldsymbol{\beta})\big) \\ \text{Subject to}: & (1)\text{–}(5),\ \Gamma_{\text{l-w}} \end{array} \tag{6}$$

where $U_m(\cdot)$ represents the utility of PeNB m. Note that it is important to guarantee fair spectrum sharing between LTE and Wi-Fi networks, as it has been shown in [4], [5] that the throughput of Wi-Fi networks can be considerably degraded with the presence of co-channel interference from LTE networks. Without the fairness constraint, i.e., $\Gamma_{\text{l-w}}$ in (6), the coexistence architecture will lead to maximizing the aggregate utility of the LTE/Wi-Fi networks as a whole. While this certainly makes sense if LTE and Wi-Fi networks are deployed by the same service provider, the Wi-Fi networks may suffer from low utility otherwise as the optimization gives higher priority in spectrum access to LTE networks that typically has higher spectral efficiency than Wi-Fi.

IV. Cross-Technology Fairness

To define the fairness criterion $\Gamma_{\text{l-w}}$ rigorously, we first derive the achievable throughput $R_m(\boldsymbol{\alpha},\ \boldsymbol{\beta})$ in (6) for U-LTE networks. The derivation is based on the protocol interference model in favor of practical LTE network management,

while the fairness definition is based on a combination of protocol and physical interference models to characterize both opportunistic and hidden node transmission behaviors in Wi-Fi networks.

A. U-LTE Throughput

We characterize as in [16], [17] the interference relationship among LTE Pico cells based on the protocol interference model. Then, the transmission collisions among LTE Pico cells in $\mathcal{M}$ can be represented using a conflict graph $\mathcal{G} \triangleq (\mathcal{M}, \mathcal{I}(\mathcal{M}, \mathcal{M}))$, where the vertices comprise all PeNBs in $\mathcal{M}$ and interference relationship $\mathcal{I}(\mathcal{M}, \mathcal{M})$ is defined as

$$\mathcal{I}(\mathcal{M}, \mathcal{M}) \triangleq \{I(m, m') \in \{0, 1\} | m, m' \in \mathcal{M},\ m \neq m'\}, \quad (7)$$

where two pico cells m and m' are able to transmit on the same channel simultaneously without causing mutual interference if their distance $d_{\mathrm{L}}(m, m')$ is higher than a threshold d_{th}, i.e., $I(m, m') = 0$ if $d_{\mathrm{L}}(m, m') > d_{\mathrm{th}}$, and $I(m, m') = 1$ otherwise. The threshold d_{th} can be determined in an online manner for given PeNB transmission power and radio propagation environment, and the conflict graph can be constructed based on the methods discussed in Section VII.

As described in Section III, multi-channel FSA allows a channel to be assigned to more than one LTE PeNB. If a channel $f \in \mathcal{F}$ is assigned to PeNBs conflicting with each other according to conflict graph $\mathcal{G}$, the channel will be shared among the PeNBs in a Time Division Multiple Access (TDMA) fashion. Then, we have

$$(\beta_{mf} + \beta_{m'f}) I(m, m') \leq 1,\ \forall m, m' \in \mathcal{M},\ f \in \mathcal{F}, \quad (8)$$

$$(\beta_{mf} + \beta_{m'f} + \beta_{m''f}) I(m, m') I(m, m'') I(m', m'') \leq 1,\ \forall m, m', m'' \in \mathcal{M},\ f \in \mathcal{F}, \quad (9)$$

$$\cdots$$

$$\left(\sum_{m \in \mathcal{M}} \beta_{mf} \right) \prod_{I(m,m') \in \mathcal{I}} I(m, m') \leq 1, \quad (10)$$

where (8) are channel sharing constraints for all two-Pico-cell pairs, and (9) are constraints for all three-pico-cell combinations, and so forth.

Then, the throughput $R_m(\boldsymbol{\alpha}, \boldsymbol{\beta})$ achievable by LTE Pico cell $m \in \mathcal{M}$ can be expressed as

$$R_m(\boldsymbol{\alpha}, \boldsymbol{\beta}) = \left(\sum_{f \in \mathcal{F}} \beta_{mf} \right) R_m^0,\ \forall m \in \mathcal{M}, \quad (11)$$

where parameter R_m^0 represents the achievable throughput if pico cell m exclusively occupies channel f. While R_m^0 is jointly determined by transmission power of PeNB, the number and locations of UEs served by the PeNB as well as the scheduling policy, it can be measured online by dividing the achieved throughput over the spectrum access time actually available to U-LTE networks.

B. Fairness Criterion

The definition of fairness in our coexistence architecture is simple. That is, we consider the spectrum sharing between U-LTE and Wi-Fi networks to be fair if the performance degradation caused by an LTE Pico cell to the Wi-Fi network is no more than the performance degradation that would be caused by another co-located Wi-Fi network offering the same level of traffic load. Yet, however, while the criterion is intuitive, defining it rigorously is in practice nontrivial primarily because of the lack of compatibility of MAC- and PHY-layer protocols, the uncoordinated LTE and Wi-Fi networks as well as the randomness in Wi-Fi network deployments. To address the challenges, we define the criterion based on *equivalent spectrum access time reservation*, and for this purpose we first analyze the throughput achievable by each Wi-Fi network with co-channel interference from another Wi-Fi network (instead of from a LTE Pico cell).

Wi-Fi throughput with interfering Wi-Fi. Let $R_{\mathrm{w},n}^0$ and $R_{\mathrm{w},n}(n')$ represent the throughput achievable by Wi-Fi network $n \in \mathcal{N}$ without and with interference from another Wi-Fi network n', respectively. Then, $R_{\mathrm{w},n}(n')$ can be expressed as the product of $R_{\mathrm{w},n}^0$ and the percentage of air time available to Wi-Fi n, denoted as $\beta_{\mathrm{w},n}(n') \in [0,\ 1]$, i.e.,

$$R_{\mathrm{w},n}(n') = \beta_{\mathrm{w},n}(n') R_{\mathrm{w},n}^0, \quad (12)$$

with $R_{\mathrm{w},n}^0$ corresponding to air time of full spectrum access with $\beta_{\mathrm{w},n}(n') = 1$. Hence, to derive $R_{\mathrm{w},n}(n')$ we only need to derive $\beta_{\mathrm{w},n}(n')$.

We adopt a hybrid protocol and physical interference model to capture the traffic- and propagation-dependent effects of the interfering Wi-Fi network n' on $\beta_{\mathrm{w},n}(n')$, respectively. In a nutshell, based on this model the achievable air time percentage $\beta_{\mathrm{w},n}(n')$ can be expressed as

$$\beta_{\mathrm{w},n}(n') = \underbrace{\widehat{\beta}_{\mathrm{w},n}(n')}_{\substack{Protocol \\ term}} + \underbrace{\widetilde{\beta}_{\mathrm{w},n}(n')}_{\substack{Opportunistic \\ term}} - \underbrace{\overline{\beta}_{\mathrm{w},n}(n')}_{\substack{Hidden\ node \\ term}}, \quad (13)$$

where $\widehat{\beta}_{\mathrm{w},n}(n')$ represents the air time percentage of spectrum access achievable with protocol interference model, and $\widetilde{\beta}_{\mathrm{w},n}(n')$ represents the percentage through opportunistic channel access under physical interference model, and $\overline{\beta}_{\mathrm{w},n}(n')$ represents the probability of channel access collisions caused by hidden node transmissions [18]. While $\widehat{\beta}_{\mathrm{w},n}(n')$ primarily depends on the traffic load ratio between two Wi-Fi networks, $\widetilde{\beta}_{\mathrm{w},n}(n')$ and $\overline{\beta}_{\mathrm{w},n}(n')$ are mainly affected by the signal propagation environment together with network topology.

First, based on protocol interference model and setting infinite interference range, then all transmissions of the interfering Wi-Fi network n' can be perfectly sensed by Wi-Fi n. Further let all Wi-Fi stations have the same opportunity to access the channel, by setting the same contention window size for them in CSMA. Then, the percentage of spectrum access time available to Wi-Fi network n can be expressed as

$$\widehat{\beta}_{\mathrm{w},n}(n') = \frac{\text{WiFi } n \text{ STAs plus AP}}{\text{All STAs plus two APs}} = \frac{|\mathcal{W}_n|_{\mathrm{up}} + 1}{|\mathcal{W}_n|_{\mathrm{up}} + |\mathcal{W}_{n'}|_{\mathrm{up}} + 2}, \quad (14)$$

and $1 - \widehat{\beta}_{\mathrm{w},n}(n')$ for Wi-Fi n'. Here, $|\mathcal{W}_n|_{\mathrm{up}}$ and $|\mathcal{W}_{n'}|_{\mathrm{up}}$ count the number of Wi-Fi stations in $\mathcal{W}_n$ and $\mathcal{W}_{n'}$ that have data to transmit in uplinks (i.e., to AP), respectively. The resulting $\widehat{\beta}_{\mathrm{w},n}(n')$ needs to be calibrated (as discussed below) to account for the effects of radio signal propagation, since in real networks the interference range causing harmful effects is finite only.

Then, based on physical interference model, the opportunistic term $\widetilde{\beta}_{\mathrm{w},n}(n')$ in (13) can be written as

$$\widetilde{\beta}_{\mathrm{w},n}(n') = \underbrace{(1-\widehat{\beta}_{\mathrm{w},n}(n'))}_{\substack{Interfering\\ Wi-Fi\ n'\ transmits}} \cdot \underbrace{\eta_{\mathrm{w},n}(n')}_{\substack{Wi-Fi\ n\ transmits\\ oppunistically}} \quad (15)$$

where $\eta_{\mathrm{w},n}(n')$ represents the channel access probability of Wi-Fi n with an ongoing interfering transmission in Wi-Fi n'. Let P_{w} represent the transmission power of each Wi-Fi AP, $H_{\mathrm{w},n}(n')$ and $h_{\mathrm{w},n}(n')$ represent the experienced path loss and channel fading coefficient from AP n' to n, and P_{th} the channel detection threshold above which a channel is sensed to be busy and sensed to be idle otherwise, then $\eta_{\mathrm{w},n}(n')$ can be expressed as

$$\begin{aligned}\eta_{\mathrm{w},n}(n') &= prob\big[P_{\mathrm{w}}H_{\mathrm{w},n}(n')h_{\mathrm{w},n}(n') \le P_{\mathrm{th}}\big] \\ &= prob\left[h_{\mathrm{w},n}(n') \le \frac{P_{\mathrm{th}}}{P_{\mathrm{w}}H(d_{\mathrm{w}}(n,n'))}\right], \end{aligned} \quad (16)$$

where $H_{\mathrm{w},n}(n') = H(d_{\mathrm{w}}(n,n'))$ with $d_{\mathrm{w}}(n,n')$ being the distance between Wi-Fi APs n and n'.

Finally, when Wi-Fi network n is transmitting (with probability $\widehat{\beta}_{\mathrm{w},n}(n')$ in (14)), the interfering Wi-Fi network n' may also access the channel opportunistically. The corresponding probability, denoted as $\widetilde{\beta}_{\mathrm{w},n'}(n)$, can be calculated similarly as $\widetilde{\beta}_{\mathrm{w},n}(n')$ in (15). If the opportunistic access causes sufficiently high interference at Wi-Fi n, transmission collision occurs (i.e., hidden node collision). Again, if we use detection threshold P_{th} as an indication of high and low interference, the collision probability denoted as $\overline{\eta}_{\mathrm{w},n}(n')$ is then

$$\overline{\eta}_{\mathrm{w},n}(n')=prob\big[P_{\mathrm{w}}H_{\mathrm{w},n}(n')h_{\mathrm{w},n}(n') > P_{\mathrm{th}}\big]=1-\eta_{\mathrm{w},n}(n'), \quad (17)$$

and the hidden-node term $\overline{\beta}_{\mathrm{w},n}(n')$ in (13) can be given as

$$\overline{\beta}_{\mathrm{w},n}(n') = \underbrace{\widehat{\beta}_{\mathrm{w},n}(n')}_{\substack{Wi-Fi\ n\\ transmits}} \cdot \underbrace{\widetilde{\beta}_{\mathrm{w},n'}(n)}_{\substack{Wi-Fi\ n'\\ opportunistic\\ access}} \cdot \underbrace{\overline{\eta}_{\mathrm{w},n}(n')}_{\substack{High\\ interference}} \quad (18)$$

where the three items at the right-hand side represent the probability that Wi-Fi n transmits (given in (14)), the interfering Wi-Fi n' opportunistically access the channel, and their transmissions collide at Wi-Fi n, respectively.

Spectrum access time reservation with interfering LTE. So far we have obtained the percentage of spectrum access time available to Wi-Fi n, i.e., $\beta_{\mathrm{w},n}(n')$ in (13), by considering that the interferer is another Wi-Fi network n'. Now we replace Wi-Fi n' with an LTE Pico cell m which accesses channel f_n (i.e., the channel used by Wi-Fi network n) in β_{mf_n} portion of air time as defined in (3)-(5). Then, the percentage of spectrum access time available to Wi-Fi n, denoted as $\beta_{\mathrm{w},n}(m)$, can be calculated as

$$\beta_{\mathrm{w},n}(m) = \underbrace{1-\beta_{mf_n}}_{LTE\ muted} + \underbrace{\beta_{mf_n}\widetilde{\beta}_{\mathrm{w},n}(m)}_{\substack{Wi-Fi\ opportunistic\\ transmission}}, \quad (19)$$

where $1-\beta_{mf_n}$ is the percentage of air time in which LTE is muted, and $\beta_{mf_n}\widetilde{\beta}_{\mathrm{w},n}(m)$ is the probability that Wi-Fi n is able to access the channel opportunistically with $\widetilde{\beta}_{\mathrm{w},n}(m)$ being calculated similarly as in (15).

Recall at the beginning of Section IV-B that, the rationale of cross-technology fairness $\Gamma_{\mathrm{l-w}}$ is to ensure that an LTE Pico cell does not degrade Wi-Fi network n more than the interfering Wi-Fi n'. Therefore we have

$$\beta_{\mathrm{w},n}(m) \ge \beta_{\mathrm{w},n}(n') \Rightarrow \beta_{mf_n} \le \frac{1-\beta_{\mathrm{w},n}(n')}{1-\widetilde{\beta}_{\mathrm{w},n}(m)}, \quad (20)$$

with $\beta_{\mathrm{w},n}(m)$ and $\beta_{\mathrm{w},n}(n')$ given in (19) and (13), respectively. Moreover, based on multi-channel FSA in Section III, channel f_n can be assigned to multiple LTE Pico cells and shared among them in a TDMA manner. Intuitively, a Pico cell located far from Wi-Fi n should be allocated more air time on channel f_n since it causes lower-level interference, and less and even zero air time of spectrum access for nearby Pico cells. To account for this intuition, we first obtain $\beta_{\mathrm{w},n}(n' \triangleq m)$ for all Pico cells $m \in \mathcal{M}$ according to (13), and then obtain again the percentage of air time that should be reserved for Wi-Fi network n by calculating a weighted summation of $\beta_{\mathrm{w},n}(n' \triangleq m)$, denoted by $\beta_{\mathrm{w},n}$, as

$$\beta_{\mathrm{w},n} = \sum_{m\in\mathcal{M}} \beta^2_{\mathrm{w},n}(n' \triangleq m) \Big/ \sum_{m\in\mathcal{M}} \beta_{\mathrm{w},n}(n' \triangleq m), \quad (21)$$

where $\beta_{\mathrm{w},n}(n' \triangleq m)$ means calculating $\beta_{\mathrm{w},n}(n')$ according to (13) by deploying the interfering Wi-Fi n' at LTE Pico cell $m \in \mathcal{M}$. Then, the constraints in (19) and (20) can be rewritten as

$$\underbrace{1-\sum_{m\in\mathcal{M}}\beta_{mf_n}}_{LTE\ muted} + \underbrace{\sum_{m\in\mathcal{M}}\beta_{mf_n}\widetilde{\beta}_{\mathrm{w},n}(m)}_{\substack{Wi-Fi\ opportunistic\\ transmission}} \ge \beta_{\mathrm{w},n}. \quad (22)$$

In (21) if Pico cell m is located closer to Wi-Fi n it results in a smaller $\beta_{\mathrm{w},n}(n' \triangleq m) \in [0,\ 1]$ and hence is less weighted; $\beta_{\mathrm{w},n}$ reduces to $\beta_{\mathrm{w},n}(n' \triangleq m)$ if Pico cell m is the only interferer.

Summary: So far, we have presented the CU-LTE coexistence architecture and the associated cross-technology fairness criterion. To study how the coexisting LTE and Wi-Fi networks interact with each other in spectrum sharing based on the coexistence architecture, next we solve the resulting fairness constrained network utility maximization problem and analyze their spectrum access behaviors based on the optimization results.

V. Utility Maximization

To be concrete, we consider individual utility function $U_m \triangleq \log(\cdot)$ in (6), which introduces proportional fairness among LTE Pico cells. The utility maximization problem (6) can then be rewritten as

$$\begin{array}{ll} \text{Given :} & \mathcal{M}, \mathcal{N}, \mathcal{L}_m, \mathcal{W}_n,\ \mathcal{G},\ \beta_{\mathrm{w},n},\ \forall m \in \mathcal{M}, n \in \mathcal{N} \\ \underset{\boldsymbol{\alpha},\,\boldsymbol{\beta}}{\text{Maximize}} & U \triangleq \sum\limits_{m\in\mathcal{M}} \log\big(R^0_m \sum\limits_{f\in\mathcal{F}} \beta_{mf}\big) \\ \text{Subject to :} & (1)-(5), (7)-(22). \end{array} \quad (23)$$

The resulting problem is a mixed integer nonlinear optimization problem (MINLP), because channel assignment variables $\alpha_{mf},\ m \in \mathcal{M}, f \in \mathcal{F}$, take only binary values in constraints (1), (2) and (5). Given an arbitrary such problem, there are no existing algorithms to obtain the global optimum with

polynomial computational complexity with respect to the number of integer variables. In this work, we design a solution algorithm *based on a combination of branch and bound and successive convex relaxation techniques* to decide the optimal channel access profile (in the sense satisfying certain predefined optimality precision) for the coexisting LTE/Wi-Fi networks.

Overall algorithm. Denote the globally optimal objective function of problem (23) as $U^\star$. Then the algorithm is designed to search for spectrum access profiles $\boldsymbol{\alpha}$ and $\boldsymbol{\beta}$ so that the achieved network utility U satisfies $U \geq \varepsilon U^\star$, with $\varepsilon \in (0, 1]$ being certain predefined optimality ratio. To this end, the algorithm iteratively maintains a global upper bound $\overline{U}_{\rm glb}$ and a global lower bound $\underline{U}_{\rm glb}$ on U, with $\underline{U}_{\rm glb} \leq U^\star \leq \overline{U}_{\rm glb}$. The algorithm also maintains a set of sub-problems of the original optimization problem (23). Denote the set of feasible sets of the resulting subproblems as $\widetilde{\Upsilon} = \{\Upsilon_i |\ i = 1, 2, \cdots\}$, with Υ_i representing the feasible set of sub-problem i.

The algorithm is initialized by setting $\underline{U}_{\rm glb} = -\infty$, $\overline{U}_{\rm glb} = +\infty$ and $\widetilde{\Upsilon} = \{\Upsilon_0\}$, where Υ_0 represents the feasible set of the original optimization problem (23). Then, Υ_0 is partitioned into two subsets Υ_1 and Υ_2, with $\Upsilon_1, \Upsilon_2 \subset \Upsilon_0$ and $\Upsilon_1 \cup \Upsilon_2 = \Upsilon_0$. For each new subset $\Upsilon_i, i = 1, 2$, the algorithm calculates a local upper bound $\overline{U}_{\rm lcl}(\Upsilon_i)$ through *convex relaxation* and a local lower bound $\underline{U}_{\rm lcl}(\Upsilon_i)$ through *local search*. After the first iteration, $\widetilde{\Upsilon}$ is updated as $\widetilde{\Upsilon} = \{\Upsilon_1, \Upsilon_2\}$. The subset partition procedures proceed iteratively, and in each iteration the algorithm selects a subset from $\widetilde{\Upsilon}$, partitions the selected subset into two new smaller subsets, and then calculates the local and upper bounds over each of them. After each iteration, the algorithm updates the global upper and lower bounds as

$$\overline{U}_{\rm glb} = \max_{\Upsilon_i \in \widetilde{\Upsilon}} \{\overline{U}_{\rm lcl}(\Upsilon_i)\}, \tag{24}$$

$$\underline{U}_{\rm glb} = \max_{\Upsilon_i \in \widetilde{\Upsilon}} \{\underline{U}_{\rm lcl}(\Upsilon_i)\}, \tag{25}$$

and the algorithm terminates if $\underline{U}_{\rm glb} \geq \varepsilon \overline{U}_{\rm glb}$ is satisfied.

In each iteration, we select subset $\Upsilon_i \in \widetilde{\Upsilon}$ for further partition such that the local upper bound $\overline{U}_{\rm lcl}(\Upsilon_i)$ of the corresponding subproblem is the highest among all the subsets in $\widetilde{\Upsilon}$, i.e., $i = \arg\max_i \overline{U}_{\rm lcl}(\Upsilon_i)$, and partition Υ_i by fixing a channel assignment variable α_{mf} to $\alpha_{mf} = 0$ and $\alpha_{mf} = 1$. Next, we describe the convex relaxation and the local search methods.

Convex relaxation. The objective of convex relaxation is to obtain a local upper bound for each selected subproblem. To this end, we obtain a fractional spectrum access (FSA) profile $\boldsymbol{\beta}$ by solving (23) *without* considering constraints (1) and (2) and *with* α_{mf} set to 1 in (5), i.e., by allowing each LTE PeNB to operate on up to $F_{\max} = |\mathcal{F}|$ channels simultaneously. The resulting optimization problem is convex, since the utility function U in (23) is concave with respect to β_{mf}, and the feasible set defined through (3)-(5), (8)-(10), (20) and (22) is convex. Consequently, the global optimum of the convexified MINLP can be obtained efficiently using standard convex optimization techniques, e.g., interior point methods [19]. Denote the resulting optimal FSA profile $\boldsymbol{\beta}$ as $\boldsymbol{\beta}^\star \triangleq (\beta^\star_{mf})_{m \in \mathcal{M}, f \in \mathcal{F}}$, based on which we can obtain a channel selection profile $\boldsymbol{\alpha}^\star = (\alpha^\star_{mf})_{m \in \mathcal{M}, f \in \mathcal{F}}$ with $\alpha^\star_{mf} = 1$ if $\beta^\star_{mf} > 0$, and $\alpha^\star_{mf} = 0$ otherwise. The corresponding aggregate utility provides an upper bound on the objective function U of the current subproblem.

Local search. Based on the obtained optimal solution of the relaxed convex optimization problem, the number of channels assigned to Pico cell $m \in \mathcal{M}$, denoted as $F^\star_m$, can be represented as

$$F^\star_m = \sum_{f \in \mathcal{F}} \alpha^\star_{mf},\ \forall m \in \mathcal{M}. \tag{26}$$

If $F^\star_m \leq F_{\max}$ for all Pico cells $m \in \mathcal{M}$, $\boldsymbol{\alpha}^\star$ and $\boldsymbol{\beta}^\star$ are the optimal solutions to the original MINLP (23); otherwise, we adjust the channel assignment for Pico cells that have been assigned more than $F_{\max}$ channels. Denote the corresponding set of Pico cells as $\mathcal{M}' = \{m | m \in \mathcal{M},\ F^\star_m > F_{\max}\}$, and let $\mathcal{F}_m \triangleq \{f | f \in \mathcal{F},\ \beta^\star_{mf} > 0\}$ represent the set of channels assigned to each PeNB $m \in \mathcal{M}'$. Without loss of generality, further let

$$\beta^\star_{mf_1} \geq \beta^\star_{mf_2} \geq \cdots \geq \beta^\star_{mf_{F_{\max}}} \geq \cdots \geq \beta^\star_{mf_{F^\star_m}}, \tag{27}$$

with $f_k \in \mathcal{F}_m,\ \forall k = 1, \cdots, F^\star_m$. Then, let PeNB $m^\star \in \mathcal{M}'$ operate on channels $f_k \in \mathcal{F}_{m^\star}$ with $k \leq F_{\max}$, with PeNB m^* determined according to

$$m^\star = \arg\max_{m \in \mathcal{M}'} \sum_{k=1}^{F_{\max}} \beta^\star_{mf_k}. \tag{28}$$

The rationale behind (27) and (28) is to fix the channel selection profile for the PeNB corresponding to the most deterministic FSA profile. This results in two additional constraints on the channel selection profile $\boldsymbol{\alpha}$ and FSA profile $\boldsymbol{\beta}$,

$$\alpha_{m^\star f_k} = 0,\ \forall f_k \in \mathcal{F}_{m^\star},\ k > F_{\max}, \tag{29}$$

$$\beta_{m^\star f_{k'}} \geq \beta^\star_{m^\star f_{k'}},\ \forall f_{k'} \in \mathcal{F}_{m^\star},\ k' \leq F_{\max}, \tag{30}$$

which means that PeNB $m^\star$ *should not* be assigned channel f_k any more and *should* be assigned at least $\beta^\star_{m^\star f_{k'}}$ spectrum access time on channel $f_{k'}$ in the following channel assignment adjustment. Constraints (29) and (30) are then incorporated into (23), and the procedure of *convex relaxation* and *local search* is repeated until the carrier aggregation constraint (2) is satisfied by all LTE Pico cells $m \in \mathcal{M}$. The resulting aggregate utility is used to serve as a local lower bound on the objective function U of the current subproblem.

Theorem 1: Given a spectrum sharing problem (23) with global optimum $U^\star$ and any predefined optimality precision $\varepsilon \in (0,\ 1]$, the algorithm always achieves aggregate network utility U that satisfies $U \geq \varepsilon U^\star$.

Proof: The proof follows the fact that, in the designed solution algorithm only binary channel assignment variables α_{mf} are partitioned while the operation is not needed for fractional spectrum variables β_{mf}. This implies that, in the worst case, the algorithm ends up with a maximum number $2^{|\mathcal{F}| \cdot |\mathcal{M}|}$ of subproblems. In each subproblem i the channel assignment variables are all fixed to either $\alpha_{mf} = 0$ or $\alpha_{mf} = 1$, and the resulting subproblem is convex with respect to fractional spectrum access variables β_{mf} and hence there is *no* gap between the calculated local upper bound $\overline{U}_{\rm lcl}(\Upsilon_i)$ and

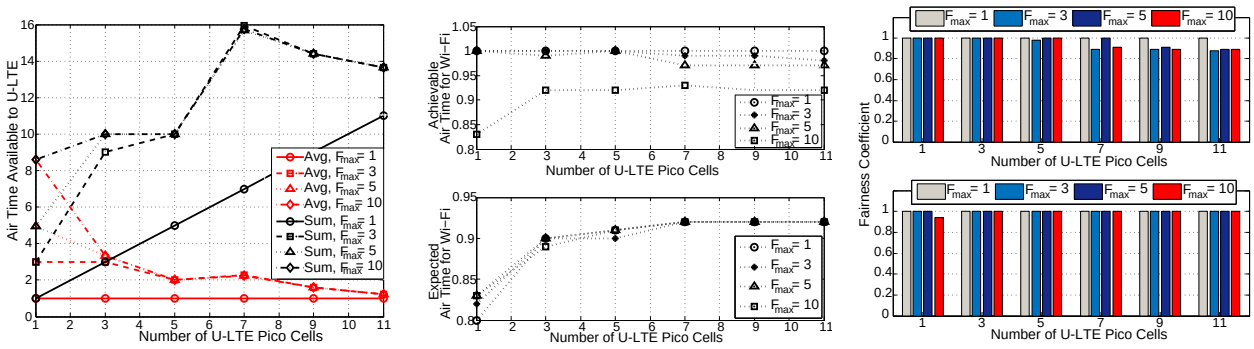

(a) (b) (c)

Fig. 3: Spectrum assignment with different number of LTE Pico cells. (a) Average and sum air time achievable by LTE; (b) achievable and expected air time for Wi-Fi; and (c) intra-system fairness coefficient of U-LTE (top) and Wi-Fi (bottom) networks.

the lower bound $\underline{U}_{\rm lcl}(\Upsilon_i)$. According to the update criterion in (24) and (25), the global upper bound $\overline{U}_{\rm glb}$ and the global lower bound $\underline{U}_{\rm glb}$ can be guaranteed to converge to each other, and hence the predefined optimality condition $U \geq \varepsilon U^\star$ can be satisfied. The tradeoff between utility optimality and computational complexity can be achieved by terminating the algorithm once the optimality condition is satisfied. Further, to speedup convergence of the algorithm, a subset Υ_i will be removed from $\widetilde{\Upsilon}$ if the resulting local upper bound satisfies $\overline{U}_{\rm lcl}(\Upsilon_i) < \underline{U}_{\rm glb}$, which implies that it is impossible to attain the global optimum of the original problem (23) by further partitioning subset Υ_i. Details of the proof are omitted due to limit of space. ■

VI. Performance Evaluation

Consider a coexisting wireless networks with a communication area $300 \times 300\text{m}^2$, 10 randomly located (with uniform distribution) Wi-Fi networks, and 1∼11 uniformly deployed LTE Pico cells, and up to ten channels (3 in 2.4 GHz band and 7 in 5 GHz band). The maximum number of channels each LTE PeNB is able to operate on simultaneously is set to $F_{\max} = 1,\ 3,\ 5,\ 10$. Uplink/downlink traffic ratio is set to 0.25 for each Wi-Fi network, and U-LTE/Wi-Fi traffic ratio is set to 0.15∼1.6 with step 0.3. The transmission power of all nodes, channel detection threshold, and the power density of AGWN are set to typical values 17 dBm, -82 dBm and -92 dBm/Hz, respectively. Path loss model

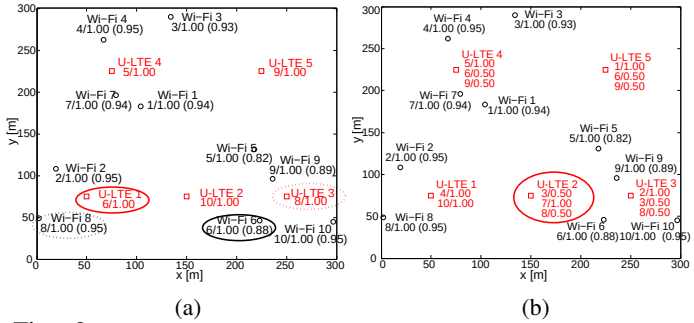

(a) (b)

Fig. 2: Channel assignment (a) without and (b) with carrier aggregation. U-LTE: channel assigned/FSA; Wi-Fi: channel assigned/achievable FSA (expected FSA).

TABLE I: Spectrum assignment without (top row) and with (bottom row) carrier aggregation.

#	LTE 1	LTE 2	LTE 3	Wi-Fi 3	Wi-Fi 4	Wi-Fi 5
1	3/1.00	1/1.00	8/1.00	1.00(0.89)	1.00 (0.94)	1.00 (0.94)
	2/0.46 3/0.57 7/0.46	2/0.54 3/0.43 7/0.54	1/1.00 8/0.33 10/1.00	0.92 (0.89)	1.00 (0.94)	1.00 (0.94)
2	8/1.00	6/1.00	7/1.00	1.00 (0.94)	1.00 (0.89))	1.00 (0.95)
	1/0.50 9/0.50 10/0.50	3/0.33 5/1.00 8/1.00	1/0.50 9/0.50 10/0.50	1.00 (0.94)	0.94 (0.89))	1.00 (0.95)
3	6/1.00	10/1.00	9/1.00	1.00 (0.95)	1.00 (0.94))	1.00 (0.88)
	3/0.50 4/0.50 5/0.50	6/0.67 7/0.67 10/1.00	1/1.00 6/0.33 8/1.00	1.00 (0.95)	1.00 (0.94))	1.00 (0.88)
4	7/0.57	10/1.00	5/1.00	1.00 (0.95)	1.00 (0.94))	0.87 (0.87) **Wi-Fi 7**
	2/0.67 8/1.00 9/0.67	3/0.50 4/0.50 10/0.50	3/0.50 4/0.50 10/0.50	1.00 (0.95)	1.00 (0.94))	1.00 (0.87) **Wi-Fi 7**
5	2/1.00	10/1.00	8/1.00	1.00 (0.86)	1.00 (0.88))	1.00 (0.95)
	2/1.00 4/1.00 6/0.33	1/0.47 5/0.47 10/0.56	6/0.67 8/0.67 9/1.00	1.00 (0.95)	1.00 (0.94))	0.99 (0.88)

is $L = 37 + 30\log 10(d)$ with d being distance in meter [20], multipath fading is set as in [4] to be Rayleigh.

Case study. We first examine two examples of spectrum access in Fig. 2, where there are five LTE Pico cells and 10 Wi-Fi networks, and U-LTE/Wi-Fi traffic ratio is set to 1. In Fig. 2(a) each LTE PeNB is configured to operate on only one channel (i.e., no carrier aggregation), and we plot the channel assignment results for each LTE Pico cell and each Wi-Fi, and the corresponding fractional spectrum access (FSA) coefficient as well as the expected FSA coefficient. One can see that, based on the proposed coexistence scheme all LTE Pico cells are able to operate on a channel with full spectrum access (i.e., $\beta_{mf} = 1$), e.g., LTE 1 on channel 6 coexisting with Wi-Fi 6 while LTE 3 on channel 8 coexisting with Wi-Fi 8. Through dynamic channel selection, each resulting coexisting LTE/Wi-Fi pair are located sufficiently far from each other, and consequently all Wi-Fi networks also achieve full spectrum access.

In Fig. 2(b), carrier aggregation is enabled by allowing each LTE PeNB to operate on up to three channels simultaneously (i.e., $F_{\max} = 3$). It can be seen that all LTE Pico cells achieve air time of spectrum access twice of that without carrier aggregation (i.e., in total 2.00 against 1.00), while *not* degrading the performance of Wi-Fi networks. For example,

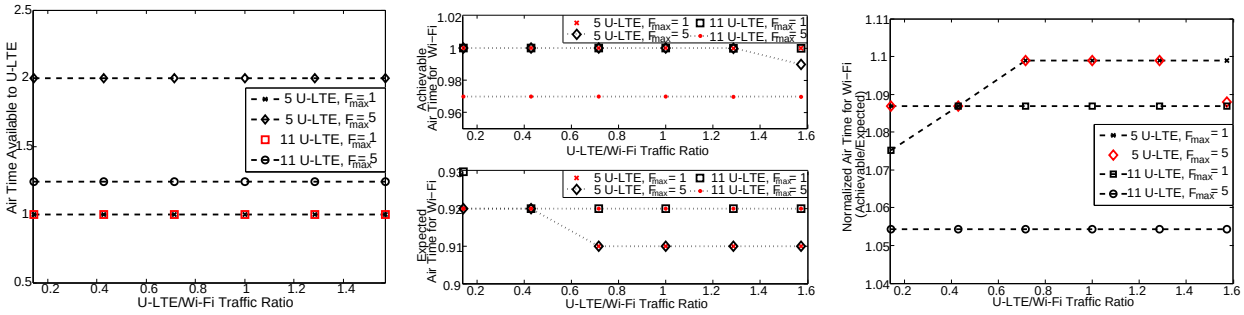

(a) (b) (c)

Fig. 4: Spectrum assignment with different LTE/Wi-Fi traffic ratio. (a) Achievable air time for LTE, (b) achievable and expected air time for Wi-Fi, and (c) normalized air time of Wi-Fi.

LTE 2 operates on channel 3 with FSA coefficient 0.5, and 1.0 and 0.5 on channels 7 and 8, respectively. More examples are given in Table I, where the spectrum access results are reported for LTE networks 1, 2 and 3 (out of 5 networks) and for Wi-Fi networks 3, 4 and 5 (out of 10 in total). Similarly, compared to the case without carrier aggregation (row 1 of each example), with carrier aggregation the spectrum access time is considerably increased for all LTE networks without any noticeable degradation to Wi-Fi performance. Particularly, in example #4, without carrier aggregation LTE 1 and Wi-Fi 7 achieve spectrum access time 0.57 and 0.87, respectively, where 0.87 is the minimum air time guaranteed by the cross-technology fairness criterion; with carrier aggregation enabled, both the two networks harvest more spectrum access time, which are increased by 2.34 (0.67+1.0+0.67) and 1.0, respectively. In all the tested instances, we found that fair spectrum access between LTE and Wi-Fi networks can be always guaranteed based on the proposed coexistence architecture.

Optimality and fairness. In Fig. 3 we plot the channel assignment results against the number LTE Pico cells. From Fig. 3(a) one can see that, considerable gain in terms of spectrum access time can be achieved with carrier aggregation, while the gain decreases as more LTE Pico networks are deployed. With densely deployed Pico cells, which is 5 in Fig. 3(a), there is no need to aggregate more than three channels.

The spectrum access time achievable by Wi-Fi networks is plotted in Fig. 3(b). From the bottom figure one can see that, somewhat surprisingly, the Wi-Fi networks harvest more spectrum access time with more interfering LTE Pico cells deployed in the coexistence area. The intuition behind is like this. Based on the definition of the cross-technology fairness criterion in Section IV, the expected spectrum access time for Wi-Fi networks is calculated according to (21) and this enforces that a Pico cell causing higher interference to Wi-Fi networks (hence smaller $\beta_{\mathrm{w},n}(m)$) is less weighted in (21). Consequently, the coexistence scheme can avoid causing catastrophic performance degradation to Wi-Fi networks in the case that the LTE service providers selfishly deploy many Pico cells. The top figure shows that the inter-system fairness can be well guaranteed in all cases. The corresponding intra-system fairness (Jain's fairness index) is plotted in Fig. 3(c), with top figure for LTE and bottom for Wi-Fi networks.

In Fig. 4 we present the channel assignment results with different LTE/Wi-Fi traffic load ratios. One can find in Fig. 4(a) that increasing the LTE traffic load does not necessarily lead to more spectrum access time for LTE networks; correspondingly, as in Figs. 4(b) and (c) the Wi-Fi performance is degraded only slightly. Again, this is because nearby interfering LTE Pico cells are only lightly weighted by the cross-technology fairness criterion. Therefore, the coexistence architecture is effective in preventing LTE SPs from aggressively offloading traffic to unlicensed bands.

Finally, we verify the optimality of the coexistence architecture in Fig. 5, by comparing it to the global optimum obtained by enumerating all possible combinations of channel assignments. A communication area of $150 \times 150\mathrm{m}^2$ with 3 Wi-Fi networks considered. Results are obtained by considering no carrier aggregation and aggregating two channels for 1, 2 and 3 co-located LTE networks. From Fig. 5(a) one can see that the proposed solution algorithm achieves the global optimum in nearly all tested instances with 3 LTE Pico cells and $F_{\max} = 2$ while in Fig. 5(b) the performance difference compared to the global optimum is negligible on average.

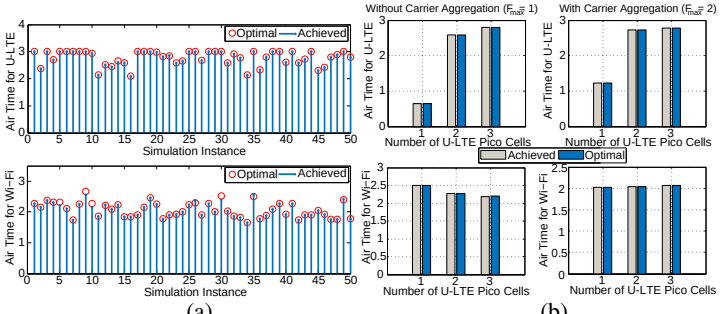

(a) (b)

Fig. 5: Channel assignments compared to the global optimum.

VII. Discussion: Applicability Issues

In this part we show that the proposed CU-LTE coexistence scheme is amenable to implementation in a cognitive manner that requires *no* signaling exchange between the coexisting LTE and Wi-Fi networks. In real networks, the spectrum access optimization can be conducted in a host server equipped with powerful computing and storage capability. The host server may be located at the LTE Macro eNodeB or a Mobility Management Entity/Service Gateway (MME/S-GW) to oversee tens and up to hundreds U-LTE Pico cells. Functionalities that run in the host server include i) calculating the spectrum access

time that should be reserved for the coexisting Wi-Fi networks according to the approach discussed in Section IV, and ii) running the optimization solution algorithm in Section V to maximize the utility of the U-LTE networks.

The spectrum access optimization requires the host server to know the traffic information of the coexisting Wi-Fi networks. This can be accomplished through packet sniffing based on *Smartphone-based crowdsourcing*, a new emerging network measurement technology [21]. As experimentally verified in [22], [23], a set of smartphones equipped with LTE/Wi-Fi dual radio interfaces can be used to overhear the packets sent by the Wi-Fi networks without actually connecting to the networks, as required by the cognitive spectrum sharing in our coexistence scheme. The overheard Wi-Fi information is sent to the host server and then used there to calculate the optimal FSA profile $\beta^\star$. The optimization results are then fed to the Macro eNodeB, which then generates ABSF patterns by configuring each subframe to be blank subframe following probability profile $\beta^\star$. The distribution of the ABSF configuration results from the Macro eNodeB to the PeNBs within its service coverage can be conducted via the X2 interface provided in 3GPP Rel. 10 [1].

The host server also needs to construct the conflict-graph of the LTE networks. This can be accomplished with different methods, e.g., distance-based criteria [24], method based on the received signal strength (RSS) [25], measurement-based RF propagation model method [26], and the online calibration method recently proposed in [27]. Particulary, in [27] the RSS measurement is conducted through a set of pre-deployed static sensors, which requires extra hardware deployment, and this restriction can be relaxed by taking the advantages of the sensing capability of smartphones to measure the RSS map.

VIII. Conclusions

We have presented CU-LTE, a new coexistence scheme to enable spectrally-efficient and fair spectrum sharing between LTE and Wi-Fi networks in the same unlicensed bands. We modeled the spectrum sharing problem as a fairness constrained mixed integer nonlinear optimization problem, and then designed an algorithm based on a combination of branch and bound and successive convex relaxation techniques to solve the problem with guaranteed optimality. Performance evaluation showed that the coexistence scheme achieves near-optimal spectrum access for U-LTE networks with always guaranteed fairness between U-LTE and Wi-Fi. Based on CU-LTE, the coexistence requires *no* signaling exchange between the coexisting networks and hence is amenable to practical applications.

References

[1] 3GPP TS 36.300 version 10.2.0 Release 10. [Online]. Available: http://www.3gpp.org/dynareport/36300.htm

[2] "Extending LTE Advanced to Unlicensed Spectrum," *Qualcomm Incorporated White Paper*, pp. 1–12, December 2013.

[3] "U-LTE: Unlicensed Spectrum Utilization of LTE," *Huawei Technology Co. Ltd. White Paper*, pp. 1–20, 2014.

[4] A. M. Cavalcante, E. Almeida, R. D. Vieira, F. Chaves, R. C. D. Paiva, F. Abinader, S. Choudhury, E. Tuomaala, and K. Doppler, "Performance Evaluation of LTE and Wi-Fi Coexistence in Unlicensed Bands," in *Proc. of IEEE VTC-Spring*, Dresden, Germany, June 2013.

[5] E. Almeida, A. M. Cavalcante, R. C. D. Paiva, F. S. Chaves, F. M. A. Jr., R. D. V. S. Choudhury, E. Tuomaala, and K. Doppler, "Enabling LTE/WiFi Coexistence by LTE Blank Subframe Allocation," in *Proc. of IEEE ICC*, Budapest, Hungary, June 2013.

[6] R. Ratasuk, M. A. Uusitalo, N. Mangalvedhe, A. Sorri, S. Iraji, C. Wijting, and A. Ghosh, "License-Exempt LTE Deployment in Heterogeneous Network," in *Proc. of ISWCS*, Paris, France, August 2012.

[7] T. Nihtila, V. Tykhomyrov, O. Alanen, M. A. U. A. Sorriy, M. Moisioy, S. Irajix, R. Ratasukz, and N. Mangalvedhez, "System Performance of LTE and IEEE 802.11 Coexisting on a Shared Frequency Band," in *Proc. of IEEE WCNC*, Shanghai, China, April 2013.

[8] S. S. Sagari, "Coexistence of LTE and WiFi Heterogeneous Networks via Inter Network Coordination," in *Proc. of MobiSys PhD Forum*, Bretton Woods, NH, June 2014.

[9] S. Yun and L. Qiu, "Supporting WiFi and LTE Co-existence," in *Proc. of IEEE INFOCOM*, Hong Kong S.A.R., PRC, April 2015.

[10] P. Kulkarni, W. H. Chin, and T. Farnham, "Radio Resource Management Considerations for LTE Femto Cells," *ACM SIGCOMM Computer Communication Review*, vol. 40, no. 1, pp. 126–30, January 2010.

[11] M. Cierny, H. Wang, R. Wichman, Z. Ding, and C. Wijting, "On Number of Almost Blank Subframes in Heterogeneous Cellular Networks," *IEEE Trans. on Wireless Comm.*, vol. 12, no. 10, pp. 5061–5073, Oct. 2013.

[12] J. B. Rao and A. O. Fapojuwo, "A Survey of Energy Efficient Resource Management Techniques for Multicell Cellular Networks," *IEEE Communications Surveys & Tutorials*, vol. 16, no. 1, pp. 154–180, FIRST QUARTER 2014.

[13] C.-F. Chiasserini and R. R. Rao, "Coexistence Mechanisms for Interference Mitigation in the 2.4-GHz ISM Band," *IEEE Trans. on Wireless Communications*, vol. 2, no. 5, pp. 964–975, September 2003.

[14] X. Zhang and K. G. Shin, "Enabling Coexistence of Heterogeneous Wireless Systems: Case for ZigBee and WiFi," in *Proc. of ACM MobiHoc*, Paris, France, May 2011.

[15] P. Guo, J. Cao, K. Zhang, and X. Liu, "Enhancing Zigbee Throughput Under WiFi Interference Using Real-time Adaptive Coding," in *Proc. of IEEE INFOCOM*, Toronto, Canada, April 2014.

[16] K. Jain, J. Padhye, V. N. Padmanabhan, and L. Qiu, "Impact of Interference on Multi-hop Wireless Network Performance," in *Proc. of ACM MobiCom*, San Diego, California, September 2003.

[17] M. Kodialam and T. Nandagopal, "Characterizing the Capacity Region in Multi-Radio Multi-Channel Wireless Mesh Networks," in *Proc. ACM MobiCom*, Cologne, Germany, August 2005.

[18] S. Xu and T. Saadawi, "Does the IEEE 802.11 MAC Protocol Work Well in Multihop Wireless Ad Hoc Networks?" *IEEE Communications Magazine*, vol. 39, no. 6, pp. 130–137, June 2001.

[19] Y. E. Nesterov and A. S. Nemirovskii, *Interior Point Polynomial Algorithms in Convex Programming*. SIAM: Philadelphia, 2004.

[20] 3GPP TR 25.942 V10.0.0, "Radio Frequency (RF) system scenarios," 3rd Generation Partnership Project, Technical Specification Group Radio Access Networks, Technical Report, 2011.

[21] A. Faggiani, E. Gregori, L. Lenzini, V. Luconi, and A. Vecchio, "Smartphone-Based Crowdsourcing for Network Monitoring: Opportunities, Challenges, and a Case Study," *IEEE Communications Magazine*, vol. 52, no. 1, pp. 106–113, January 2014.

[22] S. Sen, J. Yoon, J. Hare, J. Ormont, and S. Banerjee, "Can They Hear Me Now?: A Case for a Client-assisted Approach to Monitoring Wide-area Wireless Networks," in *Proc. of ACM SIGCOMM Conference on Internet Measurement*, Berlin, Germany, November 2011.

[23] J. Shi, Z. Guan, C. Qiao, T. Melodia, D. Koutsonikolas, and G. Challen, "Crowdsourcing Access Network Spectrum Allocation Using Smartphones," in *Proc. ACM HotNets*, Los Angeles, California, Oct. 2014.

[24] M. Alicherry, R. Bhatia, and L. E. Li, "Joint Channel Assignment and Routing for Throughput Optimization in Multi-radio Wireless Mesh Networks," in *Proc. ACM MobiCom*, Cologne, Germany, August 2005.

[25] M. C. Necker, "Towards Frequency Reuse 1 Cellular FDM/TDM Systems," in *Proc. ACM/IEEE MSWiM*, Malaga, Spain, October 2006.

[26] J. Robinson, R. Swaminathan, and E. W. Knightly, "Assessment of Urban-scale Wireless Networks With a Small Number of Measurements," in *Proc. ACM MobiCom*, San Francisco, California, Sept. 2008.

[27] X. Zhou, Z. Zhang, G. Wang, X. Yu, B. Y. Zhao, and H. Zheng, "Practical Conflict Graphs for Dynamic Spectrum Distribution," in *Proc. ACM SIGMETRICS*, Pittsburgh, PA, June 2013.